Geophysical Journal International

Geophys. J. Int. (2015) **202,** 1843–1847
GJI Seismology

doi: 10.1093/gji/ggv255

EXPRESS LETTER

Seismic attenuation due to heterogeneities of rock fabric and fluid distribution

Jing Ba,[1,2] José M. Carcione[3] and Weitao Sun[4]

[1]*School of Mathematics and Statistics, Xi'an Jiaotong University,* 710049 *Xi'an, China. E-mail: jba@uh.edu*
[2]*Department of Earth and Atmospheric Sciences, University of Houston, Houston, TX* 77204, *USA*
[3]*Istituto Nazionale di Oceanografia e di Geofisica Sperimentale (OGS), Borgo Grotta Gigante* 42c, *Sgonico, Trieste I-*34010, *Italy*
[4]*Zhou Pei-Yuan Center for Applied Mathematics, Tsinghua University,* 100083 *Beijing, China*

Accepted 2015 June 10. Received 2015 June 9; in original form 2015 March 24

SUMMARY

The study of the influence of rock fabric and porefluid distribution on the seismic wavefield is important for the prediction and detection of reservoir properties such as lithology and fluid saturation. Wave-induced local fluid flow (WILFF), which is affected by local heterogeneities of the pore structure and fluid saturation, is believed to be the main mechanism to explain the measured attenuation levels at different frequency bands. These two types of heterogeneity affect seismic waves as a combined WILFF process. In this work, we consider a double-porosity system, each part with a different compressibility and patchy saturation, and derive the wave equations from Hamilton's principle. A plane-wave analysis yields the properties of the classical *P*-wave and those of the four slow waves. The examples show that patchy fluid saturation dominates the peak frequency of the relaxation mechanism. The relation between seismic anelasticity (velocity dispersion and attenuation) and saturation depends on frequency and on the geometrical features of the two heterogeneities. The proposed theory constitutes the comprehensive description for wave propagation process through reservoirs rocks of shallow Earth and porous media in general, to estimate fluid content and distribution.

Key words: Microstructures; Permeability and porosity; Elasticity and anelasticity; Seismic attenuation; Wave propagation; Acoustic properties.

1 INTRODUCTION

It is currently accepted that seismic attenuation in earth rocks is closely related to the presence of pore fluids. The so-called 'local fluid flow' mechanism controlled by rock structure heterogeneity has been widely discussed in the literature (Mavko & Nur 1975; Dvorkin & Nur 1993; Dvorkin *et al.* 1995; Pride *et al.* 2004; Carcione & Picotti 2006; Ba *et al.* 2008), where a single fluid saturates the rock but different compressibility of pore systems induce fluid pressure diffusion in wave oscillations, leading to acoustic loss (Fig. 1a). Chapman (2009) modelled wave dispersion and attenuation controlled by the mesoscale fractures in porous rock, which may support attempts to differentiate open and closed fractures based on seismic responses. Ba *et al.* (2011) derived the wave motion governing equations in a mesoscopically heterogeneous rock, which is constituted of two components with different compressibility. Quintal *et al.* (2011) calculated frequency-dependent seismic attenuation due to WILFF in porous media with mesoscale heterogeneities by using quasi-static creeping test method. Rubino *et al.* (2013) investigated the effect of fracture connectivity on WILFF and the relevant attenuation, where additional attenuation produced by flow within connected fractures is observed.

On the other hand, patchy fluid saturation also yields WILFF (White 1975; Johnson 2001; Müller *et al.* 2010), where immiscible fluids saturate a single-porosity medium (see Fig. 1b) and compressibility contrasts between different fluid zones cause attenuation. Caspari *et al.* (2011) modelled the velocity-saturation relation with continuous random-media theories of patchy saturation and estimated *in situ* CO_2 patchy size. Masson & Pride (2011) used the invasion percolation model to build virtual rock samples saturated in patches with two immiscible fluids and then modelled seismic attenuation numerically. Sun *et al.* (2014) compared the theoretical models of *P*-wave attenuation of patchy-saturation with experimental velocity-saturation relations of different rock types. Ba *et al.* (2015) considered wave-velocity dispersion caused by fluid distribution in rock physics modelling to estimate the *in situ* porosity and hydrocarbon saturation of carbonate gas reservoirs.

Theoretical studies are reported either for the case of pore structure heterogeneity with a single fluid saturation or for a single-porosity system with patchy saturation, however they cannot model the wave propagation process in real rocks where two types of

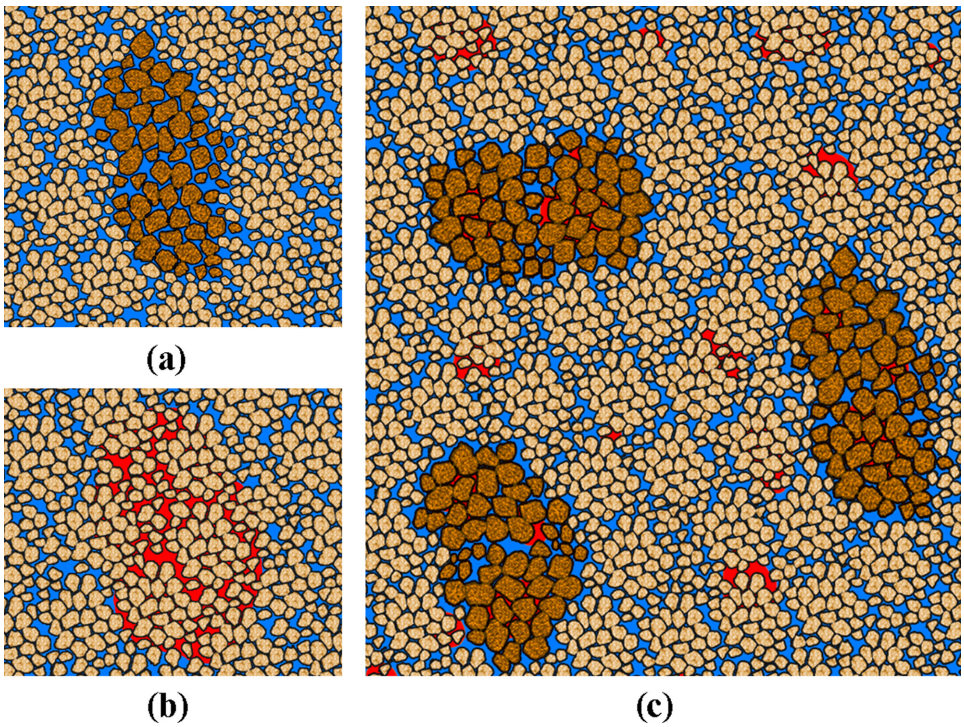

Figure 1. Synoptic diagram showing typical rock fabrics and fluid saturation: (a) heterogeneity of pore structure with a single fluid; (b) patchy-saturation heterogeneity (two immiscible fluids) in a homogeneous pore structure; (c) superposition of the two types of heterogeneity.

heterogeneity coexist. Recent experimental studies (Sharma *et al.* 2013; Lopes *et al.* 2014) have shown that acoustical loss in patchy/partially saturated rocks should also be related to the internal variations of the rock fabric/structure. The theories need to be generalized to analyse the overlapping effect of the two types of heterogeneity.

The most common case is that illustrated in Fig. 1c (sand grain sorting results in pore structure heterogeneity in the aggregates; fluids migration and accumulation cause patchy-saturation), where the two types of heterogeneity overlap and patchy-saturation occurs in each component. In this work, we investigate the effects of the two heterogeneities on wave propagation, based on poroelasticity theory, where a double double-porosity model is designed to describe the superposition of the two heterogeneities. The wave propagation theory is derived from the Hamilton's principle. Wave dispersion and attenuation are then analysed by a plane-wave analysis.

2 WAVE PROPAGATION THEORY IN DOUBLE DOUBLE-POROSITY MEDIUM

A theory was developed to analyse the WILFF mechanism in a double-porosity medium saturated with a single fluid, in which the equations of motion are derived from Hamilton's principle by assuming porous spherical inclusions embedded in a single-porosity host (Ba *et al.* 2011). In this work we consider the case shown in Fig. 1(c), assuming that the frame and fluid patches are spherical, and patchy saturation occurs in both the inclusion and the host medium (Fig. 2a).

Since the two porous components have different local porosities, permeability and capillary forces, fluid patches from different components have dissimilar properties. We assume that all the inclusions are spherical with radius R_{12}, where subscripts 1 and 2 indicate host and inclusion, respectively. Furthermore, fluid patches in the host and inclusion frames have the radii R_{13} and R_{24}, respectively, where subscripts 3 and 4 indicate the fluid patches in the host and inclusion, respectively.

When seismic waves squeezes the medium, the compressibility contrasts between different zones induce WILFF at the surface of the discontinuities. We denote by ς_{12}, ς_{13} and ς_{24} the fluid strain increment in the WILFF process at the different types of boundaries. The Biot strain potential energy is given by

$$\begin{aligned} 2W = {} & (A+2N)e^2 - 4N(e_{11}e_{22} - e_{12}^2 + e_{22}e_{33} - e_{23}^2 + e_{11}e_{33} \\ & - e_{13}^2) + 2Q_1 e(\xi_1 + \phi_2\varsigma_{12} + \phi_3\varsigma_{13}) + R_1(\xi_1 + \phi_2\varsigma_{12} \\ & + \phi_3\varsigma_{13})^2 + 2Q_2 e(\xi_2 - \phi_1\varsigma_{12} + \phi_4\varsigma_{24}) + R_2(\xi_2 - \phi_1\varsigma_{12} \\ & + \phi_4\varsigma_{24})^2 + 2Q_3 e(\xi_3 - \phi_1\varsigma_{13}) + R_3(\xi_3 - \phi_1\varsigma_{13})^2 \\ & + 2Q_4 e(\xi_4 - \phi_2\varsigma_{24}) + R_4(\xi_4 - \phi_2\varsigma_{24})^2, \end{aligned} \tag{1}$$

where ϕ_1, ϕ_2, ϕ_3 and ϕ_4 are the porosities of the four zones in the proposed double double-porosity system and ξ_1, ξ_2, ξ_3 and ξ_4 are the corresponding pore fluid bulk strains. Moreover, $e_{ij}, i, j = 1, 2, 3$ are the strain components of the solid and e is the solid bulk strain. The stiffnesses A, N, Q_1, Q_2, Q_3, Q_4, R_1, R_2, R_3 and R_4 can be determined by means of 'gedanken' experiments in terms of the rock-frame and fluid physical properties (Biot & Willis 1957; Johnson 1986).

On the basis of the Biot–Rayleigh theory (Ba *et al.* 2011), the kinetic energy of the system is

$$\begin{aligned} 2T = {} & \rho_{00}(\dot{u}_1^2 + \dot{u}_2^2 + \dot{u}_3^2)^2 + 2\rho_{01}(\dot{u}_1\dot{U}_1^{(1)} + \dot{u}_2\dot{U}_2^{(1)} + \dot{u}_3\dot{U}_3^{(1)}) \\ & + 2\rho_{02}(\dot{u}_1\dot{U}_1^{(2)} + \dot{u}_2\dot{U}_2^{(2)} + \dot{u}_3\dot{U}_3^{(2)}) + 2\rho_{03}(\dot{u}_1\dot{U}_1^{(3)} + \dot{u}_2\dot{U}_2^{(3)} \\ & + \dot{u}_3\dot{U}_3^{(3)}) + 2\rho_{04}(\dot{u}_1\dot{U}_1^{(4)} + \dot{u}_2\dot{U}_2^{(4)} + \dot{u}_3\dot{U}_3^{(4)}) \\ & + \rho_{11}(\dot{U}_1^{(1),2} + \dot{U}_2^{(1),2} + \dot{U}_3^{(1),2}) + \rho_{22}(\dot{U}_1^{(2),2} + \dot{U}_2^{(2),2} + \dot{U}_3^{(2),2}) \\ & + \rho_{33}(\dot{U}_1^{(3),2} + \dot{U}_2^{(3),2} + \dot{U}_3^{(3),2}) + \rho_{44}(\dot{U}_1^{(4),2} + \dot{U}_2^{(4),2} + \dot{U}_3^{(4),2}) \end{aligned}$$

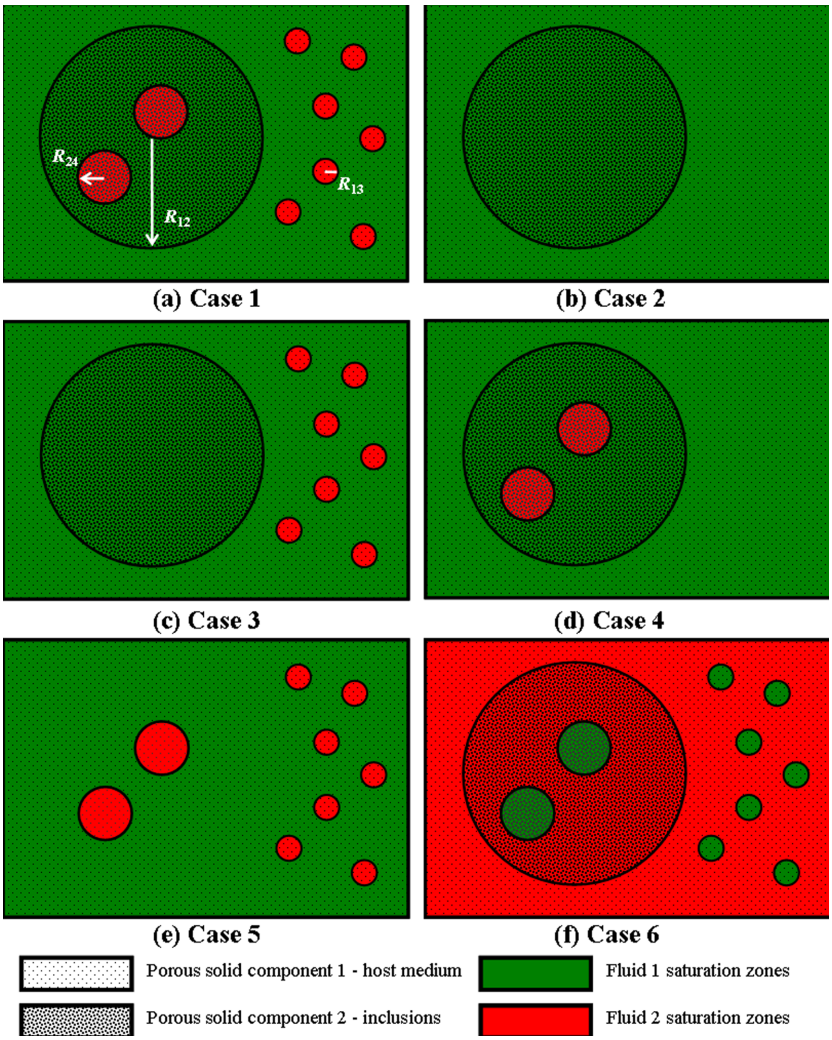

Figure 2. Six cases of superposed heterogeneities of frame and fluid patches.

$$+\frac{1}{3}\rho_f^{(1)}\dot{\varsigma}_{12}^2 R_{12}^2\frac{\phi_1^2\phi_2^2\phi_{20}}{\phi_{10}(\phi_2+\phi_4)}+\frac{1}{3}\rho_f^{(1)}\dot{\varsigma}_{13}^2 R_{13}^2\phi_1^2\phi_3$$
$$+\frac{1}{3}\rho_f^{(1)}\dot{\varsigma}_{24}^2 R_{24}^2\phi_2^2\phi_4, \tag{2}$$

where $\mathbf{u}=[u_1,u_2,u_3]$ is the displacement vector of the rock solid frame, $\mathbf{U}^{(m)}=[U_1^{(m)},U_2^{(m)},U_3^{(m)}]$ $(m=1,2,3,4)$ is the pore fluid displacement vector in the four zones and $\rho_f^{(1)}$ and $\rho_f^{(2)}$ are the mass densities of the two immiscible fluids, inside and outside the patches, respectively. The density coefficients ρ_{00}, ρ_{01}, ρ_{02}, ρ_{03}, ρ_{04}, ρ_{11}, ρ_{22}, ρ_{33} and ρ_{44} can be determined as a function of the porosities, tortuosities, saturations and solid and fluid densities (Biot 1962). Moreover, ϕ_{10} and ϕ_{20} are the local porosities of the inclusion and host, respectively.

The dissipation functions in WILFF can be derived in the same way,

$$D=\frac{1}{2}\sum_m b_m(\mathbf{u}-\mathbf{U}^{(m)})\cdot(\mathbf{u}-\mathbf{U}^{(m)})+\frac{1}{6}\eta^{(1)}\dot{\varsigma}_{12}^2 R_{12}^2\frac{\phi_1^2\phi_2^2\phi_{20}}{\kappa_1(\phi_2+\phi_4)}$$
$$+\frac{1}{6}\eta^{(1)}\dot{\varsigma}_{13}^2 R_{13}^2\frac{\phi_3\phi_1^2\phi_{10}}{\kappa_1}+\frac{1}{6}\eta^{(1)}\dot{\varsigma}_{24}^2 R_{24}^2\frac{\phi_4\phi_2^2\phi_{20}}{\kappa_2}, \tag{3}$$

where b_m are the Biot diffusion coefficients of the different zones (Biot 1962), which depend on the fluid viscosities, frame permeabilities and porosities.

The equations of motion can be obtained from Hamilton's principle. It yields

$$\begin{aligned}&N\nabla^2\mathbf{u}+(A+N)\nabla e+Q_1\nabla(\xi^{(1)}+\phi_2\varsigma_{12}+\phi_3\varsigma_{13})\\&\quad+Q_2\nabla(\xi^{(2)}-\phi_1\varsigma_{12}+\phi_4\varsigma_{24})+Q_3\nabla(\xi^{(3)}-\phi_1\varsigma_{13})\\&\quad+Q_4\nabla(\xi^{(4)}-\phi_2\varsigma_{24})\\&=\rho_{00}\ddot{\mathbf{u}}+\rho_{01}\ddot{\mathbf{U}}^{(1)}+\rho_{02}\ddot{\mathbf{U}}^{(2)}+\rho_{03}\ddot{\mathbf{U}}^{(3)}+\rho_{04}\ddot{\mathbf{U}}^{(4)}\\&\quad+b_1(\dot{\mathbf{u}}-\dot{\mathbf{U}}^{(1)})+b_2(\dot{\mathbf{u}}-\dot{\mathbf{U}}^{(2)})\\&\quad+b_3(\dot{\mathbf{u}}-\dot{\mathbf{U}}^{(3)})+b_4(\dot{\mathbf{u}}-\dot{\mathbf{U}}^{(4)})\end{aligned} \tag{4}$$

$$\begin{aligned}&Q_1\nabla e+R_1\nabla(\xi^{(1)}+\phi_2\varsigma_{12}+\phi_3\varsigma_{13})\\&\quad=\rho_{01}\ddot{\mathbf{u}}+\rho_{11}\ddot{\mathbf{U}}^{(1)}-b_1(\dot{\mathbf{u}}-\dot{\mathbf{U}}^{(1)})\end{aligned}$$

$$\begin{aligned}&Q_2\nabla e+R_2\nabla(\xi^{(2)}-\phi_1\varsigma_{12}+\phi_4\varsigma_{24})\\&\quad=\rho_{02}\ddot{\mathbf{u}}+\rho_{22}\ddot{\mathbf{U}}^{(2)}-b_2(\dot{\mathbf{u}}-\dot{\mathbf{U}}^{(2)})\end{aligned}$$

$$Q_3\nabla e+R_3\nabla(\xi^{(3)}-\phi_1\varsigma_{13})=\rho_{03}\ddot{\mathbf{u}}+\rho_{33}\ddot{\mathbf{U}}^{(3)}-b_3(\dot{\mathbf{u}}-\dot{\mathbf{U}}^{(3)})$$

$$Q_4\nabla e+R_4\nabla(\xi^{(4)}-\phi_2\varsigma_{24})=\rho_{04}\ddot{\mathbf{u}}+\rho_{44}\ddot{\mathbf{U}}^{(4)}-b_4(\dot{\mathbf{u}}-\dot{\mathbf{U}}^{(4)})$$

$$\phi_2(Q_1 e + R_1(\xi^{(1)} + \phi_2\varsigma_{12} + \phi_3\varsigma_{13})) - \phi_1(Q_2 e + R_2(\xi^{(2)} - \phi_1\varsigma_{12} + \phi_4\varsigma_{24})) = \frac{1}{3}\rho_f^{(1)}\ddot{\varsigma}_{12}R_{12}^2\frac{\phi_1^2\phi_2^2\phi_{20}}{\phi_{10}(\phi_2+\phi_4)} + \frac{1}{3}\dot{\varsigma}_{12}R_{12}^2\frac{\eta^{(1)}\phi_1^2\phi_2^2\phi_{20}}{\kappa_1(\phi_2+\phi_4)}$$

$$\phi_3(Q_1 e + R_1(\xi^{(1)} + \phi_2\varsigma_{12} + \phi_3\varsigma_{13})) - \phi_1(Q_3 e + R_3(\xi^{(3)} - \phi_1\varsigma_{13})) = \frac{1}{3}\rho_f^{(1)}\ddot{\varsigma}_{13}R_{13}^2\phi_1^2\phi_3 + \frac{1}{3}\dot{\varsigma}_{13}R_{13}^2\frac{\eta^{(1)}\phi_1^2\phi_3\phi_{10}}{\kappa_1}$$

$$\phi_4(Q_2 e + R_2(\xi^{(2)} - \phi_1\varsigma_{12} + \phi_4\varsigma_{24})) - \phi_2(Q_4 e + R_4(\xi^{(4)} - \phi_2\varsigma_{24})) = \frac{1}{3}\rho_f^{(1)}\ddot{\varsigma}_{24}R_{24}^2\phi_2^2\phi_4 + \frac{1}{3}\dot{\varsigma}_{24}R_{24}^2\frac{\eta^{(1)}\phi_2^2\phi_4\phi_{20}}{\kappa_2}.$$

By substituting a plane *P*-wave kernel into eq. (4) (Carcione 2015), the Christoffel equation is derived. There are five solutions, which correspond to the velocities and attenuation factors of the classical *P*-wave and four Biot diffusion waves.

3 RESULTS

3.1 Frequency-dependent velocity dispersion and attenuation

Fig. 3 shows the *P*-wave velocities and attenuation for all the cases of Fig. 2, corresponding to uncemented sand inclusions (local porosity of 0.3; component concentration of 0.037; permeability of 1 D) embedded in a host consolidated sandstone (local porosity of 0.1; component concentration of 0.963; permeability of 10 mD; Pride & Berryman 2003; Ba *et al.* 2011). We assume host matrix consolidation parameter of 22. Mineral density and bulk/shear moduli are 2.65 g cm^{-3} and 38/40 GPa (quartz), respectively. The fluid 1 density/viscosity/bulk modulus are 1.04 g cm^{-3}/0.001 Pa s/2.5 GPa (water), the fluid 2 corresponding values are 0.01 g cm^{-3}/0.000022 Pa s/0.14 MPa (gas), the radii of the inclusion/host patch/inclusion patch are 20 mm/0.5 mm/2 mm, and the fluid 2 saturation in the host and inclusion are 0.05 and 0.3, respectively.

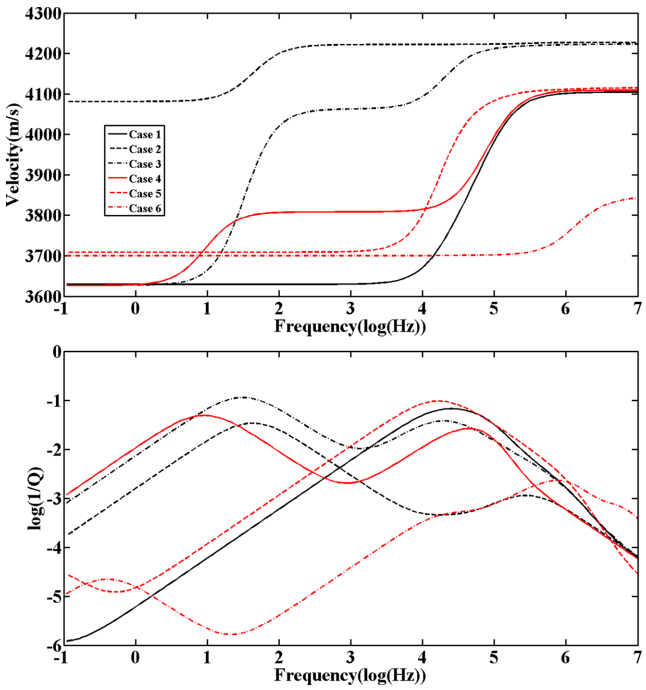

Figure 3. *P*-wave velocity (a) and attenuation (b) as a function of frequency, corresponding to a double double-porosity rock.

A comparison between Case 2 and Cases 1, 3 and 4 shows that patchy saturation in the inclusions dominates the wave velocity dispersion and attenuation. The mesoscopic inclusions in a rock fully saturated with water induce a strong attenuation peak in the seismic band (Case 2). This effect is strengthened if the host is partially saturated with gas (Case 3), where small patches in the low permeability host medium also affect seismic attenuation in the combined fluid flow. When the inclusions are patchy-saturated with gas, the combined local fluid flow causes a high attenuation peak in the ultrasonic band (Cases 1 and 4). Case 5 shows velocity dispersion and attenuation in the single-porosity host medium saturated with two sets of patches. In Case 6, the two fluids are interchanged with respect to Case 1. Both cases show no significant attenuation in the seismic band, with Case 6 having the lowest level of velocity dispersion and attenuation.

3.2 Seismic attenuation due to fluid saturation

In the double-porosity rock, we consider four different experimental methods to vary the water/gas saturation. In a drying experiment for fully water-saturated rock, water loss is dependent on the sample surface area and irrelevant with pore structures (Cadoret *et al.* 1995). It can be assumed that water loss mainly occurs in the host medium and the water content of the inclusions does not decrease until the host is dry. In an imbibition experiment by depressurization, the dry sample is immersed in a water tank, and the pressure of water was decreased, therefore bubbles escaped and water saturation increases by re-equilibrating water pressure to atmospheric pressure (Cadoret *et al.* 1995). It is assumed that two components achieve the same saturation in a mesoscopic homogeneous case. In dynamic and quasi-static injection experiments, water is injected into a dry rock with high and low injection rates (Lopes *et al.* 2014), respectively. We assume gas is injected into a fully-saturated rock with a controlled injection rate for a drained experiment. With a low injection rate in a quasi-static draining experiment, gas accumulates in the high porosity/permeability zones first (the inclusions for this example), so that the water saturation in the low porosity/permeability component will not decrease until the high porosity/permeability component is dry. In a dynamic draining experiment, the same amount of gas is injected into each component per unit rock volume so that the low-porosity zones undergo a higher increasing rate of gas saturation.

In these experimental methods, the history of saturation in each component is different although at the end the whole rock has the same saturation. Fig. 4 shows the *P*-wave attenuation as a function of water saturation, corresponding to the different methods. In the drying experiment, patchy saturation in the host medium causes significant attenuation in the seismic band, until the host is completely dry and gas enters into the inclusions. Then, wave attenuation decreases sharply as the inclusion saturation decreases. In the other three cases, seismic attenuation decreases with decreasing water saturation. In the dynamic injection experiment, the *P*-wave attenuation decreases by one order of magnitude as the gas saturation in the inclusions increases. At full water saturation, the WILFF is completely controlled by the pore structure heterogeneity and induces seismic attenuation. It is to be noted that seismic attenuation decreases sharply as gas simultaneously invades the two types of pore systems (see the imbibition and quasi-static injection experiments), and its magnitude decreases below 10^{-4} when only a small

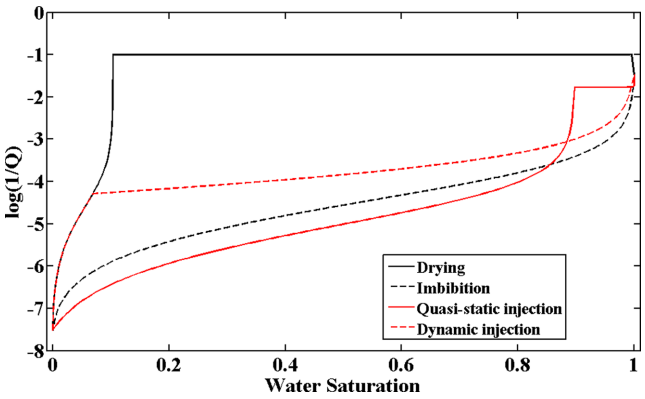

Figure 4. *P*-wave wave attenuation as a function of water saturation in the seismic band (50 Hz), corresponding to the four experimental methods.

amount of gas (<5 per cent) is present in the rock. The diffusion effect in the seismic band is weakened in the combined fluid flow process.

4 CONCLUSIONS

The effect of superposed heterogeneities of rock frame and fluid distribution on *P*-wave attenuation has been analysed by means of a novel double double-porosity model and the dynamic governing equations of wave propagation and fluid flow. Plane-wave solutions show that although the total anelastic effects are strengthened when gas invades a water-saturated double-porosity solid system, the attenuation peaks may move to high frequencies. Different features of seismic attenuation as a function of water/gas saturation can be seen in the different experimental approaches performed to vary water saturation. Seismic attenuation decreases as gas permeates the two pore systems simultaneously. Although, mesoscopic patches of rock frame and patchy saturation induce seismic attenuation, the results indicate that seismic-band loss decreases when the two heterogeneities are superposed.

In the case that light gas migrates into heterogeneous rocks, constituting gas pockets whose size is smaller than the fabric heterogeneity, the seismic intrinsic dissipation factor caused by fluid flow is not significant in general, with values of the order of 10^{-2}. To our knowledge, the theoretical method presented in this work is the first to provide a comprehensive and exact mathematic description of wave motion in real rocks. Based on rock physics modelling, the theory can be used to estimate the heterogeneity of rock frames, fluid type and distribution.

ACKNOWLEDGEMENTS

The authors are grateful to the Editor Jeannot Trampert and the anonymous reviewers for their valuable comments. This work is supported by the 'Young Talent Support Plan' of Xi'an Jiaotong University and the Fluids/DHI Consortium of UH. JB thanks Dehua Han and Hui Li for helpful discussions.

REFERENCES

Ba, J., Nie, J., Cao, H. & Yang, H., 2008. Mesoscopic fluid flow simulation in double-porosity rocks, *Geophys. Res. Lett.,* **35,** L04303, doi:10.1029/2007GL032429.

Ba, J., Carcione, J.M. & Nie, J., 2011. Biot-Rayleigh theory of wave propagation in double-porosity media, *J. geophys. Res.,* **116,** B06202, doi:10.1029/2010JB008185.

Ba, J., Du, Q., Carcione, J.M., Zhang, H. & Müller, T.M., 2015. *Seismic Exploration of Hydrocarbons in Heterogeneous Reservoirs: New Theories, Methods and Applications,* Elsevier, 292 pp.

Biot, M.A., 1962. Mechanics of deformation and acoustic propagation in porous media, *J. appl. Phys.,* **33,** 1482–1498.

Biot, M.A. & Willis, D.G., 1957. The elastic coefficients of the theory of consolidation, *ASME J. appl. Mech.,* **24,** 594–601.

Cadoret, T., Marion, D. & Zinszner, B., 1995. Influence of frequency and fluid distribution on elastic wave velocities in partially saturated limestones, *J. geophys. Res.,* **100,** 9789–9803.

Carcione, J.M., 2015. *Wave Fields in Real Media: Theory and Numerical Simulation of Wave Propagation in Anisotropic, Anelastic, Porous and Electromagnetic Media,* 3rd edn, Elsevier.

Carcione, J.M. & Picotti, S., 2006. *P*-wave seismic attenuation by slow-wave diffusion. Effects of inhomogeneous rock properties, *Geophysics,* **71,** O1–O8.

Caspari, E., Müller, T.M. & Gurevich, B., 2011. Time-lapse sonic logs reveal patchy CO_2 saturation in-situ, *Geophys. Res. Lett.,* **38,** L13301, doi:10.1029/2011GL046959.

Chapman, M., 2009. Modeling the effect of multiple sets of mesoscale fractures in porous rocks on frequency-dependent anisotropy, *Geophysics,* **74,** D97–D103.

Dvorkin, J. & Nur, A., 1993. Dynamic poroelasticity: a unified model with the Squirt and the Biot mechanisms, *Geophysics,* **58,** 524–533.

Dvorkin, J., Mavko, G. & Nur, A., 1995. Squirt flow in fully saturated rocks, *Geophysics,* **60,** 97–107.

Johnson, D.L., 1986. Recent developments in the acoustic properties of porous media, in *Frontiers in Physical Acoustics,* Vol. XCIII, pp. 255–290, eds Sette, D., Elsevier.

Johnson, D.L., 2001. Theory of frequency dependent acoustics in patchy-saturated porous media, *J. acoust. Soc. Am.,* **110,** 682–694.

Lopes, S., Lebedev, M., Müller, T.M., Clennell, M.B. & Gurevich, B., 2014. Forced imbibition into a limestone: measuring *P*-wave velocity and water saturation dependence on injection rate, *Geophys. Prospect.,* **62,** 1126–1142.

Masson, Y.J. & Pride, S.R., 2011. Seismic attenuation due to patchy saturation, *J. geophys. Res.,* **116,** B03206, doi:10.1029/2010JB007983.

Mavko, G.M. & Nur, A., 1975. Melt squirt in the asthenosphere, *J. geophys. Res.,* **80,** 1444–1448.

Müller, T.M., Gurevich, B. & Lebedev, M., 2010. Seismic wave attenuation and dispersion resulting from wave-induced flow in porous rocks—a review, *Geophysics,* **75,** 75A147–75A164.

Pride, S.R. & Berryman, J.G., 2003. Linear dynamics of double-porosity and dual permeability materials. I. Governing equations and acoustic attenuation, *Phys. Rev. E,* **68,** 036603, doi:10.1103/PhysRevE.68.036603.

Pride, S.R., Berryman, J.G. & Harris, J.M., 2004. Seismic attenuation due to wave-induced flow, *J. geophys. Res.,* **109,** B01201, doi:10.1029/2003JB002639.

Quintal, B., Steeb, H., Frehner, M. & Schmalholz, S.M., 2011. Quasi-static finite element modeling of seismic attenuation and dispersion due to wave-induced fluid flow in poroelastic media, *J. geophys. Res.,* **116,** B1201, doi:10.1029/2010JB007475.

Rubino, J.G., Guarracino, L., Müller, T.M. & Holliger, K., 2013. Do seismic waves sense fracture connectivity?, *Geophys. Res. Lett.,* **40,** 692–696.

Sharma, R., Prasad, M., Batzle, M. & Vega, S., 2013. Sensitivity of flow and elastic properties to fabric heterogeneity in carbonates, *Geophys. Prospect.,* **61,** 270–286.

Sun, W., Ba, J., Müller, T.M., Carcione, J.M. & Cao, H., 2014. Comparison of *P*-wave attenuation models of wave-induced flow, *Geophys. Prospect.,* **63**(2), 378–390.

White, J.E., 1975. Computed seismic speeds and attenuation in rocks with partial gas saturation, *Geophysics,* **40,** 224–232.